Theory of Batchwise Centrifugal Casting

P. Maarten Biesheuvel, Arian Nijmeijer, and Henk Verweij
Laboratory for Inorganic Materials Science, Dept. of Chemical Technology, University of Twente, 7500 AE Enschede, The Netherlands

In batchwise centrifugal casting a cylindrical mold is filled with suspension and rotated rapidly around its axis. This results in the movement of the particulate phase toward the cylinder wall and the formation of a tubular cast. Theory is presented for particle transport in the suspension phase and subsequent cast growth using concepts from the related fields of centrifugal sedimentation and centrifugal separation. Most attention is given to the situation of complete mold filling, which allows for several distinct simplifications. Analytical expressions for suspension concentration and cast growth are presented for the case of unhindered settling. Numerical simulations are made for hindered settling. The outcome shows a good agreement with experiments in which homogeneous porous ceramic membrane supports are made from a submicron-sized α-alumina powder.

Introduction

The formation of a cast from a suspension of particles can be done by the removal of liquid as in filtration or by the movement of particles through the liquid because of a force acting on the particles. This latter mechanism is called *sedimentation* and is the basis of cast formation in centrifugal casting. In this process, a cylindrical mold is filled with a suspension of particles with a higher density than the matrix liquid and rotated around its center axis. Subsequently, particles start to move toward the cylinder wall due to the centrifugal force and form a cast with increasing thickness. After cast release and proper posttreatment, a firm and homogeneous tubular structure can be obtained.

Centrifugal casting as described in this article occurs in an impermeable (say metal) mold, and thus no filtration occurs. This article is furthermore confined to processes in which a cylindrical mold is rotated around its own center axis, which results in the formation of a tube. The theory presented can be modified to describe cast formation in a typical laboratory centrifuge in which the mold is rotated around an axis perpendicular to its own center axis. In that case a flat cylindrical disk will be obtained.

Centrifugal casting to produce a tubular structure is applied in several areas, for example, the production of optical telecommunication fibers (Bachmann et al., 1996), steel tubes (Northcott and Dickin, 1944; Royer, 1988; Kang and Rohatgi, 1996), polyester and polyvinyl pipes (Jones, 1994), functionally gradient metal–ceramic materials (Fukui, 1991), or porous ceramic supports for membrane applications (Nijmeijer et al., 1998). Structures made by centrifugal casting have distinct properties when compared to more traditional techniques, such as extrusion and isostatic pressing. The main advantage is the uniformity in particle packing, which results in a very homogeneous product with a higher strength and a smooth inside surface. Hong (1997) uses a discrete-element method to study uniformity in particle packing of structures produced by centrifugal casting and shows that homogeneity is increased when the cast formation rate is lowered.

A uniform particle packing results in a higher corrosion resistance in case of steel tubes, while for the production of porous ceramic membrane supports a smooth inside surface and a narrow pore-size distribution are obtained, which are essential for the quality of membranes that are deposited on this surface. A centrifuged tube shows an extremely good roundness when compared to an extruded tube, which is of importance when tubes are sealed into reactor modules (Nijmeijer et al., 1998).

Theory of centrifugal casting is related to research in the fields of centrifugal sedimentation and centrifugal separation. In centrifugal sedimentation, the objective is the clarification of slurries (Perry and Green, 1984) or the analysis of size (distribution) of macromolecules and proteins (Schachman, 1959). These latter applications have already been described thoroughly, starting with Lamm (1929), whose general ultracentrifuge equation or Lamm's equation is still the basis

Correspondence concerning this article should be addressed to H. Verweij.

of any modeling effort in this field (Bowen and Rowe, 1970). The diffusional part of this equation is sometimes neglected (Sambuichi et al., 1987, 1991), but becomes an essential part if the objective is the determination of molecular weight of polymers in solution (Bowen and Rowe, 1970). The convective part is based on sedimentation velocities measured in a gravitational field. The influence of solid-phase concentration on the sedimentation velocity is often fitted to a linear function in order to obtain analytical solutions (Fujita, 1962). The mold is always partly filled with suspension before rotation is started. This results in the development of a gas–liquid interface, a supernatant, a suspension phase, and a cake layer.

In the field of centrifugal separation much attention is paid to predicting the movement of the supernatant–suspension boundary and the suspension–cast boundary (Baron and Wajc, 1979; Anestis and Schneider, 1983; Greenspan, 1983; Schaflinger and Stibi, 1987; Ungarish, 1993, p. 75). These authors follow a more rigorous approach including secondary effects as spin-up from rest, Coriolis and inertial forces, and prograde and retrograde rotation. Particle velocities are based on Stokes' law, and correction factors for hindered settling are implemented to account for higher particle concentrations. Model predictions are in excellent agreement with some experimental results obtained by Baron and Wajc (1979) and Schaflinger and Stibi (1987). Tubes with a very smooth outside surface can be obtained when particles have a lower density than the liquid and thus sediment on an inner cylinder. This situation is described by Ungarish (1993, p. 75).

The objective of this article is the application of several concepts from centrifugal sedimentation and centrifugal separation theory to centrifugal casting for the production of tubular structures. A straightforward approach is followed, resulting in a condensed model neglecting second-order effects as caused by inertial and Coriolis forces. Stokes' law is applied for unhindered settling of particles, while the influence of particle concentration (hindered settling) is implemented using a correction factor (Concha and Almendra, 1979) that is not necessarily linear. In the former case, analytical expressions describe all process parameters, while in the latter a numerical procedure must be followed. Special attention is paid to the situation of complete mold filling, which implies that a gas–liquid surface will not evolve and neither does a supernatant phase. The theory presented is based upon monosized particles with equal densities, and thus the segregation due to a distribution in size or density is not implemented. Particle sizes as used in the literature are typically of the order of 0.5–500 μm, while the volumetric particle concentration in the suspension is between 10 and 50% (see Table 3).

Particles in suspension are stabilized by interparticle repulsive forces to prevent flocculation, which would result in a cast with nonoptimum properties. In the current work two assumptions are made relating to these forces:

- First, the interparticle forces only have a working range in the order of nanometers, and can thus be neglected when calculating particle velocities: a so-called "hard-sphere" approach is used.
- Second, high pressures develop between particles in the cast that help to overcome the interparticle forces and to move particles into their primary potential minimum where they are bound strongly. Therefore it is reasonable to assume that diffusion from the cast back into the suspension phase can be neglected.

Because of particle stabilization in suspension, a dense and noncompressible cast develops (Lange and Miller, 1987). Therefore it is not necessary to solve momentum balances over the cast as has been done by Sambuichi et al. (1987, 1991) and Tiller and Hsyung (1993) to describe cast formation from a flocculated suspension.

Theoretical Background

Introduction

Theory is presented for cast formation in a vertically upright cylinder (see Figure 1) that is rotated around its center axis ($r = 0$), which causes the heavier particle phase to move toward the cylinder wall and form a cast with increasing thickness. Gravitation is neglected as a driving force for particle movement due to the high value of the centrifugal force imposed ($\omega^2 r/g \gg 1$), and therefore only balances in radial direction are solved. Constant density of the solid and the liquid phase is assumed.

In centrifugal casting a cylindrical mold is filled to a certain extent with a suspension of particle concentration ϕ_0. When rotation is started, the suspension is distributed evenly over the tube wall, leaving a cylindrical core unfilled. Particles will move away from the gas–liquid interface r_L, leaving a supernatant phase behind (see Figure 2). While the supernatant phase is growing, a cast is formed at the cylinder wall r_0 that moves inward into the suspension. When the supernatant–suspension interface r_s reaches the suspension–cast interface r_c, cast formation ceases suddenly. However, if initially the mold had been filled completely, no supernatant phase will form and the cast formation rate decays exponentially.

In the following subsections, first an overall mass balance for the particle phase is discussed, resulting in an expression for the final cast thickness. Second, the elements necessary to describe the cast formation rate are discussed: expressions

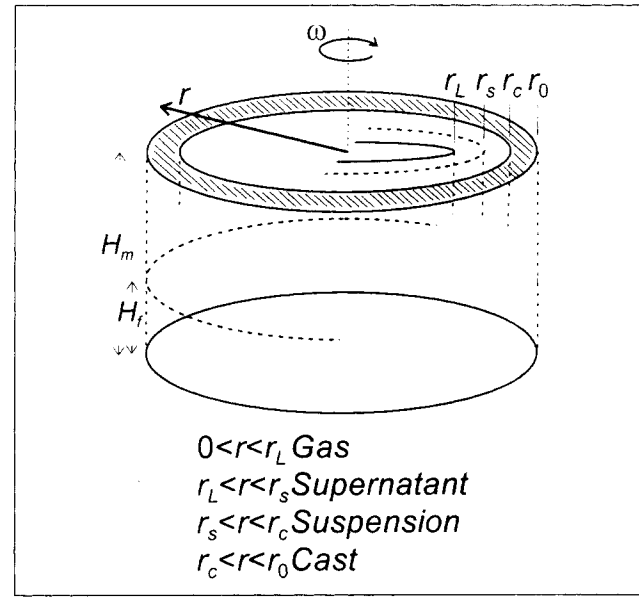

Figure 1. Centrifugal mold tube.

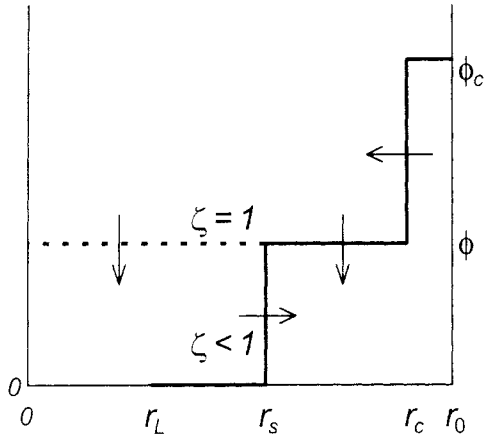

Figure 2. Concentration profiles in supernatant, suspension, and cast.

For complete filling ($\zeta = 1$, dotted line) no supernatant phase will evolve. For $\zeta < 1$ (continuous line), r_s increases from r_L at $t = 0$. Arrows indicate movement with time.

for particle velocities in the suspension phase; the equation of continuity for the suspension phase; and expressions for the movement of the suspension–cast boundary. Combination of these elements yields an expression for the rate of cast formation that is elaborated for the cases of hindered and unhindered settling and filling fractions less than and equal to unity.

Overall mass balance: final cast thickness

The final cast thickness δ_∞ can be derived from the overall mass balance for the solid phase including tube radius r_0, initial suspension concentration ϕ_0, cast concentration ϕ_c, and filling fraction ζ. Suspension and cast concentration are defined on a volume-basis. For a given amount of suspension or cast consisting of a volume solid phase V_s and liquid phase V_L, concentration ϕ is defined as

$$\phi = \frac{V_s}{V_s + V_L}. \tag{1}$$

The filling fraction ζ is defined as the ratio of total suspension volume to mold volume. If a mold with height H_m is filled to height H_f, then ζ is given by (See Figure 1):

$$\zeta = \frac{H_f}{H_m}. \tag{2}$$

After the start of rotation, liquid will overcome gravity and distribute evenly over the tube height, as far away as possible from the tube center. In the center a gas–liquid interface will develop at radius r_L, whose location can be derived from an overall mass balance for the suspension phase:

$$H_f \pi r_0^2 = H_m \pi \left(r_0^2 - r_L^2\right). \tag{3}$$

Implementation of Eq. 2 in 3 results in

$$r_L = r_0\sqrt{1-\zeta}. \tag{4}$$

The final cast thickness δ_∞ can be derived from an overall balance when all particles have been transported from the suspension into the cast and only a clear supernatant remains:

$$\pi\left\{r_0^2 - r_L^2\right\}\phi_0 = \pi\left\{r_0^2 - (r_0 - \delta_\infty)^2\right\}\phi_c. \tag{5}$$

Rearrangement of Eq. 5 and implementation of Eq. 4 results in

$$\delta_\infty = r_0\left\{1 - \sqrt{1 - \zeta\frac{\phi_0}{\phi_c}}\right\}. \tag{6}$$

Particle transport mechanisms

Transport of particles in the suspension phase is by means of convection J_c or diffusion J_d. Diffusion as a transport mechanism is not described in this article for the following reasons:

- Within the suspension no concentration gradients will develop, as will be explained later on.
- Diffusion from the cast can be neglected because of the mutual interaction of the particles within the cast, see the Introduction section.
- Diffusion from the suspension to the supernatant can be neglected for the following two reasons: 1. Particles diffusing to the supernatant will locally have a higher velocity due to the lower concentration ϕ, as is explained later on, and thus effectively move back into the suspension. 2. For high values of the Peclet number [$Pe = v \cdot L \cdot D^{-1}$ (see Westerterp et al., 1987)] diffusion can be neglected. For liquids, the diffusion coefficient D can be based on the Stokes–Einstein relation, which relates D to the Boltzmann constant k, temperature T, liquid viscosity η, and particle radius a_p:

$$D = \frac{kT}{6\pi\eta a_p}. \tag{7}$$

If length L is replaced by the tube radius r_0, the following expression for Pe can be obtained after implementation of Eqs. 14 and 7:

$$Pe = \frac{4\pi a_p^3(\rho_s - \rho_L)\omega^2 r r_0}{3kT}. \tag{8}$$

This result is analogous to Russel (1989, p. 412) for settling under gravity. For $r = r_0$ and data from Table 1, a value of $Pe = 7 \cdot 10^5$ is obtained, which implies that diffusion can be neglected.

The convective flux of particles in suspension J_c is given by the product of suspension concentration ϕ and velocity v:

$$J_c = \phi v. \tag{9}$$

The velocity v of a particle moving through a liquid under the influence of a centrifugal force field is given by a combi-

Table 1. Values as Measured and Used as Base Case in Simulations

Cast concentration (packing factor)	ϕ_c	0.55	
Initial suspension concentration	ϕ_0	0.2012	
Tube radius	r_0	0.010675	m
Particle radius	a_p	2.00×10^{-7}	m
Liquid viscosity	η	1.8×10^{-3}	Pa·s
Solid density	ρ_s	3,970	kg/m^3
Liquid density	ρ_L	1,018	kg/m^3
Angular velocity	ω	5,000 rpm = 524	rad/s
Temperature	T	300	K

nation of the centrifugal force, buoyancy, and friction. For creeping flow, the friction F_f exerted on a single sphere can be described by Stokes' law:

$$F_f = -6\pi\eta a_p v(t). \tag{10}$$

Creeping flow conditions prevail for Reynolds numbers ($= 2\rho_L v a_p \eta^{-1}$) below 0.1. A Reynolds number of $1\cdot10^{-5}$ was calculated with the data from Table 1 and with use of Eq. 14, justifying the use of Eq. 10.

In a centrifugal field, the sum of centrifugal force F_c and buoyancy F_b is described as follows, including the solid and liquid densities ρ_s and ρ_L, angular velocity ω, and radial coordinate r:

$$F_c + F_b = \frac{4}{3}\pi a_p^3(\rho_s - \rho_L)\omega^2 r. \tag{11}$$

Using Newton's second law the following second-order differential equation is obtained to describe the particle movement:

$$\frac{4}{3}\pi a_p^3(\rho_s - \rho_L)\omega^2 r - 6\pi\eta a_p \frac{dr}{dt} = \frac{4}{3}\pi a_p^3 \rho_s \frac{d^2 r}{dt^2}. \tag{12}$$

Equation 12 can only be solved in a straightforward manner if the assumption is made that the time scale on which the final particle velocity is reached is short compared to the overall process, and thus r can be looked at as a constant. In that case integration of Eq. 12 over time t results in (Ungarish, 1993, p. 27; Kang and Rohatgi, 1996):

$$v(t) = \frac{2a_p^2(\rho_s - \rho_L)\omega^2 r}{9\eta}\{1 - e^{(-9\eta t)/(2a_p^2\rho_s)}\}. \tag{13}$$

For the limit of $t \to \infty$, velocity v is given by

$$v = \frac{2a_p^2(\rho_s - \rho_L)\omega^2 r}{9\eta} = s\omega^2 r. \tag{14}$$

Here we have introduced the sedimentation coefficient s, which is used often in the literature on sedimentation and filtration. The time to reach 99% of velocity v is given by equating the ratio $v(t)/v$ with the value 0.99, which yields

$$t = -\frac{2a_p^2\rho_s}{9\eta}\ln(0.01). \tag{15}$$

For the data of Table 1, a value of $t = 9\cdot10^{-8}$ s is found. In the sequence of this article processes are in the order of seconds or larger, thus Eq. 14 can be used to describe particle velocities. Furthermore, the assumption made in the derivation of Eq. 13 proves valid.

Equation 14 is only valid for unhindered settling for a single sphere in an infinite fluidum. However, this is not generally the case, and correction factors have been determined to account for a higher concentration ϕ (Ring, 1996; Happel and Brenner, 1965; Concha and Almendra, 1979). Concha and Almendra (1979) present an overview of correction factors and arrive at a system of equations that is able to describe sedimentation satisfactorily for Reynolds numbers ranging from 10^{-3} to 10^3 and concentrations ϕ ranging from 0.01 to 0.59. In the Appendix the correction factor for hindered settling in a batch sedimentation experiment $h(\phi)$ is derived for the limiting situation of $Re \to 0$. Implementation of this expression of $h(\phi)$ in Eq. 14 results in

$$v = \frac{2a_p^2(\rho_s - \rho_L)}{9\eta}\frac{(1-\phi)(1-1.45\phi)^{1.83}}{1+0.75\phi^{1/3}}\omega^2 r = s(\phi)\omega^2 r. \tag{16}$$

It must be remarked that Eq. 16 is valid for batch sedimentation in which the particle flow induces an equal but countercurrent liquid flow. For the limiting case of $\phi \to 0$, $h(\phi)$ approaches unity, which results in unhindered settling (see Eq. 14). For $\phi \to 1$, $h(\phi)$ approaches zero and no transport will occur. Ring (1996) presents correction factors for Eq. 14 to incorporate particle asphericity. In this article a correction for asphericity is not implemented, because in the experimental work fairly spherical particles are used.

Equation of continuity for the suspension phase

The equation of continuity relates the solid-phase concentration and the convective flux and is given for cylindrical coordinates by (Lamm, 1929; Fujita, 1962; Bowen and Rowe, 1970):

$$\frac{\partial\phi}{\partial t} = -\frac{1}{r}\frac{\partial}{\partial r}(rJ_c). \tag{17}$$

Introduction of Eqs. 9 and 16 into Eq. 17 results in the following differential equation:

$$\frac{\partial\phi}{\partial t} = -2\omega^2 s(\phi)\phi - \omega^2 r\frac{\partial(s(\phi)\phi)}{\partial r}. \tag{18}$$

Sambuichi et al. (1987) showed that when the initial concentration ϕ_0 is uniform, ϕ remains independent of r for the suspension phase. Thus the second term on the righthand side of Eq. 18 will be zero and Eq. 18 simplifies to (Fujita, 1962; Bowen and Rowe, 1970; Sambuichi et al., 1987; Probstein, 1989):

$$\frac{d\phi}{dt} = -2\omega^2 s(\phi)\phi. \tag{19}$$

Boundary movement

The movement of boundaries in gravitational sedimentation has been described by Kynch (1952) and extended to centrifugal separation by Baron and Wajc (1979) and Anestis and Schneider (1983). Here, we will apply this theory exclusively for the movement of the suspension–cast boundary. The correct expression for the movement of the supernatant–suspension boundary is implicitly used in Eq. 26.

From an evaluation of the "flux vs. concentration" curve it can be foreseen whether primary discontinuities (kinematic shocks) or secondary discontinuities (kinematic waves) develop at the suspension–cast boundary (see also Russel (1989) and Probstein (1989)). In the first case, a single, sharp discontinuity develops between suspension and cast at which the particle concentration jumps from ϕ to ϕ_c. In the second case particles settle more slowly into the cast, while the suspension concentration ϕ slowly increases to ϕ_c.

In our situation, as defined by Eq. 16 and the value of ϕ_c from Table 1, only a kinematic shock develops as determined theoretically using the aforementioned flux vs. concentration curve. The change in the cast thickness δ with time t (cast growth G_c) can now be derived from a simple balance over the moving suspension–cast boundary, including the velocity of the particles in suspension at the suspension–cast boundary v_c and the velocity of particles within the cast u_c (Kynch, 1952):

$$\phi(v_c + G_c) = \phi_c(u_c + G_c). \tag{20}$$

The velocity of particles in the cast u_c is set to zero because we can assume that the cast is incompressible, see the Introduction section; thus Eq. 20 rewrites to

$$G_c = \frac{d\delta}{dt} = v_c \frac{\phi}{\phi_c - \phi}. \tag{21}$$

In the following section, several distinct cases are elaborated in which the preceding theory is applied. First of all, the situation of unhindered settling is described for filling fractions ζ equal to unity and smaller than unity. In Cases III and IV hindered settling is discussed.

Case I: $h(\phi) = 1$, $\zeta = 1$. For unhindered settling ($\{h(\phi) = 1\} \rightarrow \{s(\phi) \rightarrow s\}$), integration of Eq. 19 with the initial condition $\phi|_{t=0} = \phi_0$ results in

$$\phi = \phi_0 e^{-2s\omega^2 t}. \tag{22}$$

Implementation of Eqs. 14, 22, and the relation [$\delta = r_0 - r_c$] into Eq. 21 results, after integration with initial condition $\delta|_{t=0} = 0$, in:

$$\delta = r_0 \left\{ 1 - \sqrt{\frac{\phi_c - \phi_0}{\phi_c - \phi_0 e^{-2s\omega^2 t}}} \right\}. \tag{23}$$

This result can also be derived from an equation obtained by Ungarish (1993, p. 87) if the so-called (modified) particle Taylor number β ($= 2/9 a_p^2 \omega \rho_L \eta^{-1}$) is much smaller than unity, which is indeed the case in our situation ($\beta = 2.6 \cdot 10^{-6}$; data from Table 1). For large processing times ($t \rightarrow \infty$), Eq. 23 equals Eq. 6, which gives a check on the above derivation.

Finally, cast growth G_c is given by differentiation of Eq. 23:

$$G_c = \frac{d\delta}{dt} = r_0 s\omega^2 \phi_0 e^{-2s\omega^2 t} \frac{(\phi_c - \phi_0)^{1/2}}{\left(\phi_c - \phi_0 e^{-2s\omega^2 t}\right)^{3/2}}. \tag{24}$$

Cast formation time t_c is defined as the time to reach final cast thickness δ_∞. However, for $\zeta = 1$, t_c is infinite (see Eq. 23), thus t_c is defined as the time to reach 99% cast thickness (see also Ungarish, 1993, p. 84). Cast formation time is now derived by equating the ratio δ/δ_∞ with the value 0.99. After implementation of Eqs. 23 and 6, the following expression for t_c is obtained:

$$t_c = \frac{-1}{2s\omega^2} \ln \left(\frac{\phi_c}{\phi_0} - \frac{\frac{\phi_c}{\phi_0} - 1}{\left(0.99 \sqrt{1 - \frac{\phi_0}{\phi_c}} + 0.01 \right)^2} \right). \tag{25}$$

Cast formation time t_c is inversely proportional to the sedimentation coefficient s and has a dependence of the power -2 of the angular velocity ω. The radius of the tube r_0 has no influence on cast formation time t_c because an increase of r_0 influences the final cast thickness δ_∞ and the cast growth rate G_c in like manner. These two effects cancel out when the cast formation time is calculated. For realistic values of the suspension concentration ($0.1 < \phi_0/\phi_c < 0.6$), the entire ln part varies from 2.2 to 3.3. A change in ϕ_0 or ϕ_c thus has a less significant influence on cast formation time than a change in s or ω.

Case II: $h(\phi) = 1$, $\zeta \neq 1$. If the tube is only partially filled, a clear supernatant phase will develop. The supernatant–suspension interface r_s moves toward higher r-values until the cast surface is reached at t_c. For $t < t_c$ cast growth is equal to Case I. At t_c cast growth is suddenly reduced to zero. This behavior is in sharp contrast to Case I, where cast growth continues to decay exponentially. The movement of r_s is described by

$$\frac{dr_s}{dt} = s(\phi)\omega^2 r_s. \tag{26}$$

Integration of Eq. 26 for unhindered settling with initial condition $r_s|_{t=0} = r_L$ results in (Fujita, 1962; Probstein, 1989)

$$r_s = r_L e^{s\omega^2 t}. \tag{27}$$

Cast formation time t_c is given by the moment that the cast is reached by the supernatant phase, which is given by [$r_s = r_0 - \delta_\infty$]. After implementation of Eq. 4, the following result is obtained:

$$t_c = \frac{1}{s\omega^2} \ln \left(\sqrt{\frac{1 - \zeta\frac{\phi_0}{\phi_c}}{1 - \zeta}} \right). \tag{28}$$

From Eq. 28 it follows that for filling fractions approaching unity, the cast formation time increases to infinity ($\zeta \to 1$, $t_c \to \infty$). Implementation of Eq. 28 in Eq. 23 results in Eq. 6. Both results give a check on the validity of preceding derivations.

In Figure 2 some of the differences between Case I and Case II are summarized. As mentioned earlier, a gas phase, a supernatant, a suspension phase, and a cast layer develop for Case II (see also Probstein, 1989). For Case I only the latter two phases are present. Similar remarks on the difference between Cases I and II were made by Greenspan (1983) and Ungarish (1993, pp. 82–84).

In Figure 3 the effect of filling fraction ζ on cast growth G_c and final thickness δ_∞ is shown. Data used for this simulation are summarized in Table 1. For $t < t_c$, cast growth G_c and cast thickness δ are not influenced by ζ. Cast formation time t_c and final thickness δ_∞, however, are influenced by the filling fraction ζ. As in Case I, t_c is not influenced by r_0.

Case III: $h(\phi) \neq 1$, $\zeta = 1$. To describe higher concentrations of particles, Eq. 16 is used instead of Eq. 14, and the simplification $\{s(\phi) \to s\}$ cannot be made. For this situation, no analytical solution could be found for Eq. 19, and a numerical procedure was followed in which ϕ was determined explicitly, based on Eq. 19:

$$\phi_i = \phi_{i-1} + \Delta t^*(-2s(\phi_{i-1})\omega^2\phi_{i-1}) \tag{29}$$

Analogous to Eq. 21, cast growth G_c is given by

$$G_{c,i} = \frac{\Delta\delta_i}{\Delta t} = s(\phi_{i-1})\omega^2(r_0 - \delta_{i-1})\frac{\phi_{i-1}}{\phi_c - \phi_{i-1}}. \tag{30}$$

Cast thickness δ follows from

$$\delta_i = \delta_{i-1} + \Delta t G_{c,i}. \tag{31}$$

This set of equations can be solved with initial conditions:

$$IC: \quad t = 0 \qquad \phi_i = \phi_0 \qquad \delta_i = 0. \tag{32}$$

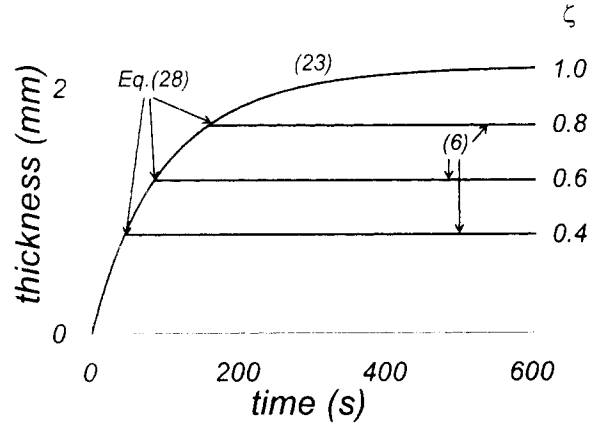

Figure 3. Cast thickness for Case I vs. Case II for different filling fractions ζ.

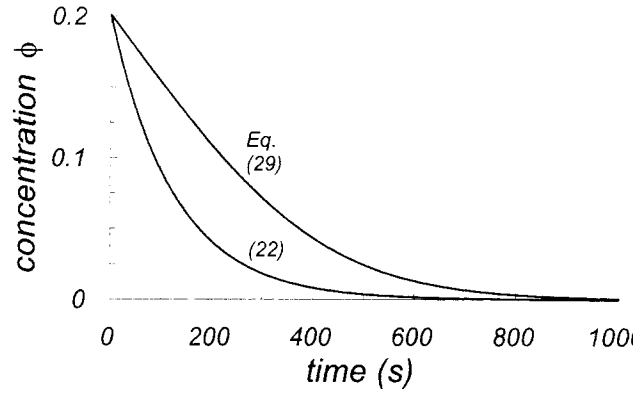

Figure 4. Suspension concentration ϕ: hindered vs. unhindered settling.

The effect of hindered settling on suspension concentration ϕ, cast growth G_c, and cast thickness δ is examined for complete mold filling ($\zeta = 1$) by comparison of Case I and Case III. If hindered settling (Case III) is compared with unhindered settling (Case I), it can be seen easily that suspension concentration decreases more slowly (Figure 4), while cast growth is lower (Figure 5). For Cases I and III, final cast thickness δ_∞ is reached for $t \to \infty$, in accordance with Eq. 6.

For different angular velocities, the cast formation time t_c is depicted in Figure 6 for complete filling ($\zeta = 1$). Irrespective of the occurrence of particle hindrance, a higher angular velocity will result in a lower t_c. For hindered settling, t_c values are higher. The influence of the initial suspension concentration ϕ_0 on t_c is different for hindered and unhindered settling (see Figure 7). On increasing ϕ_0, t_c decreases for unhindered settling due to the fact that the actual distance for a particle to travel decreases with increasing ϕ_0 because of the higher final cast thickness. For hindered settling this cannot counterbalance the effect of the decrease in the value of the correction factor $h(\phi)$.

As in Cases I and II, tube radius r_0 does not influence t_c. This result cannot be obtained easily from the equations presented but appeared from our simulations.

Case IV: $h(\phi) \neq 1$, $\zeta \neq 1$. For hindered settling and a partial mold filling, suspension concentration ϕ and cast growth G_c are described by Eqs. 29 and 30, respectively, for $t \leq t_c$.

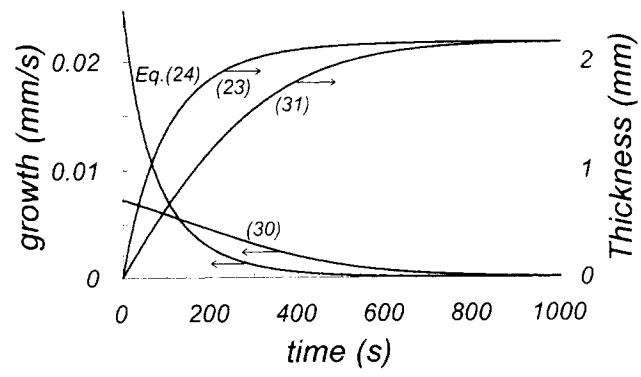

Figure 5. Cast growth and thickness: hindered vs. unhindered settling for complete filling (Cases I and III).

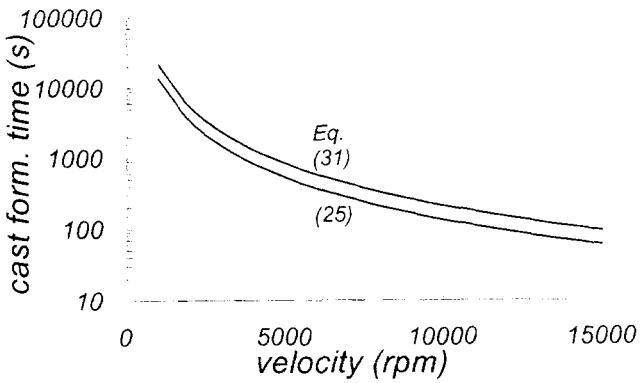

Figure 6. Cast formation time: hindered vs. unhindered settling for different angular velocities for complete filling (Cases I and III).

At $t = t_c$, supernatant reaches the cast and cast growth is reduced to zero. Cast formation time t_c can be calculated by implementation of Eq. 6 or Eq. 26 into the numerical scheme.

Experimental Studies

Nijmeijer et al. (1998) describe in detail the synthesis route to porous α-alumina membrane supports by centrifugal casting. The recipe used results in a value for the initial suspension concentration ϕ_0 of 0.2012. The viscosity η of the matrix liquid was determined in a rheometer (Contraves LS40, Mettler-Toledo AG, Greifensee, Switzerland) using a Couette geometry with radii of 5.5 and 6.0 mm. For shear rates from 10^{-1} s^{-1} to 10^{2} s^{-1}, viscosity was found to be $(1.8 \pm 0.1) \times 10^{-3}$ Pa·s. Liquid density ρ_L was obtained from a calculation based on the recipe and following the product data sheet of Darvan C (R.T. Vanderbilt Company, Inc., Norwalk, CT). Solid density ρ_s and the modal particle radius a_p were obtained directly from the α-alumina data sheet (AKP30, Sumitomo Chemical Company, Ltd., Japan) (see Table 1). A mean deviation in radius of 70 nm could be calculated from the presented size distribution. This deviation accounts for a ratio in radius of about 2 between the smaller and the larger particle fraction, and hence a ratio in the Stokes velocity of about 4. Differential settling, however, does not occur in all cases because at a higher concentration particles tend to sediment as a whole (see, e.g., Probstein, 1989). In addition, electron microscopy pictures showed no sign of size distribution in the final cast. Electron microscopy furthermore showed that particles were fairly spherical.

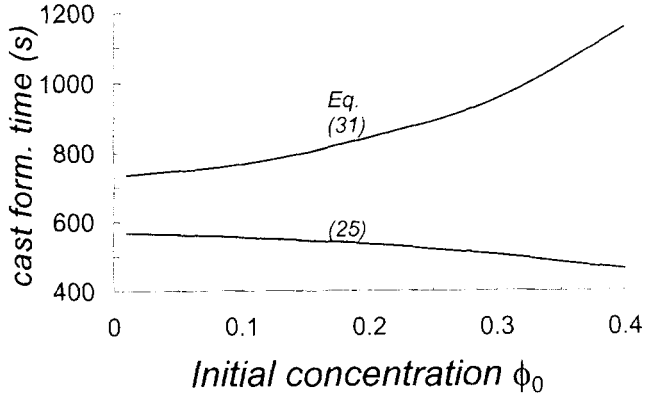

Figure 7. Cast formation time: hindered vs. unhindered settling for different initial suspension concentrations ϕ_0 for complete filling (Cases I and III).

Tubes were made as follows: 120 g of α-alumina powder was mixed with 20 mL of APMA (Ammonium PolyMethAcrylate aqueous solution, Darvan C) and 100 mL of distilled water. The mixture of water and APMA was brought on pH = 9.5 by adding NH_4OH (E. Merck, Darmstadt, Germany). The resulting mixtures were ultrasonically (Model 250 Sonifier, Branson Ultrasonics Corp., Danbury, CT) treated for 15 min with a frequency of 20 kHz and a transducer output power of 100 W. Before pouring part of the suspension into the molds, the molds were coated at the inside with Vaseline (Elida Fabergé, Bodegraven, The Netherlands) solution in petroleum ether (E. Merck, Darmstadt, Germany) (boiling range 40–60°C) as release agent. Two mold types were used with a length of 6 and 10 cm. Because the mold is rotated around its center axis, the length does not influence cast growth rates.

The tubes were centrifuged for several processing times at several angular velocities, after which the remaining liquid was poured out of the molds. The green tubes inside the molds were dried in a climate chamber (Heraus Vötch, Ballingen, Germany) for two days at 30°C and 60% relative humidity.

The cast thickness and the cast concentration (particle packing) were determined after a temperature treatment at 500°C to remove any water and dispersing agent, while the cast concentration remains the same because sintering does not occur at this temperature. The cast thickness was measured using a sliding gauge and the cast concentration was obtained using the Archimedes method by immersion of the sample in mercury.

The measured cast concentration ϕ_m changes with angular velocity ω and processing time t, see Table 2. The presented theory, however, is based on a constant cast concentration ϕ_c to simplify calculations. The measured cast thickness is therefore multiplied by the ratio of ϕ_m over ϕ_c to obtain a corrected cast thickness δ that can be compared with values obtained from simulation.

Results and Discussion

Measurements of cast thickness and cast concentration were performed for angular velocities ranging from 3,280 to

Table 2. Overview of Measurements

No.	Angular Velocity (rpm)	Process. Time (min)	Meas. Cast Conc. ϕ_m	Meas. Cast Thick. (mm)	Corrected Cast Thick. δ (mm)
1	3,278	7.5	0.5509	1.17	1.17
2	3,960	7.5	0.5329	1.32	1.28
3	4,973	7.5	0.5492	1.90	1.90
4	5,836	7.5	0.5605	2.14	2.18
5	2,522	15	0.4650	1.20	1.01
6	3,277	15	0.5536	1.64	1.65
7	3,960	15	0.5493	2.12	2.12
8	4,746	15	0.5598	2.12	2.16
9	5,836	15	0.5658	2.17	2.23

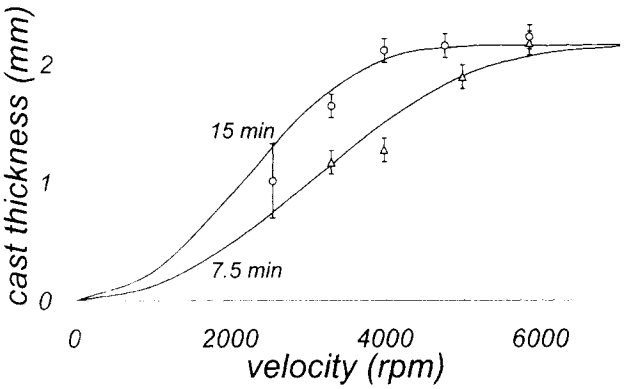

Figure 8. Cast thickness as function of angular velocity and processing time for complete filling and hindered settling (Case III).

Triangular points are measured after 7.5 min of centrifugation, circular points after 15 min. Lines are described by Eq. 31.

5,840 rpm. Casting times were either 7.5 min or 15 min. Tubes were filled completely, thus the filling fraction ζ equaled unity. Measured cast thickness ranged from 1 to 2.2 mm and cast concentration from 0.46 to 0.57. Measurement data are summarized in Table 2.

The error in cast thickness δ was ≈ 0.1 mm. In measurement No. 5 cast thickness could only be obtained by the measurement of internal and external diameter because sagging was severe. The cast was removed from the mold using a spoon and dried separately to determine the cast concentration. The error in the cast thickness was ≈ 0.3 mm.

The initial suspension is milky white and opaque. For measurements 4 and 7–9, the remaining suspension is clear. Few small particles remain. For the other measurements, the suspension remains white and opaque.

Measurements are compared with predictions for hindered settling (Case III) (see Figure 8). For the region of cast thickness increase at lower angular velocities as well as for the plateau region at higher velocities, the agreement between measurements and simulation is satisfactory. If a correction for hindered settling is not implemented, predictions for the cast thickness are higher up to a factor of 3, and thus overestimate the cast thickness significantly.

The model predicts a zero gradient for the suspension concentration. Visual observations of the suspensions when the centrifuge has ceased to rotate always agreed with this prediction: a gradient in ϕ could never be observed. Other explanations for the absence of a concentration gradient could be diffusion that equilibrates suspension concentration, or the work of turbulent eddies introduced into the suspension when the angular velocity is reduced after a certain time. From Eq. 7, however, a diffusion coefficient of 6×10^{-13} m^2/s is calculated, which cannot account for achieving equilibrium within minutes. After centrifugation, velocities were reduced to zero gradually to inhibit the introduction of turbulent eddies.

Experimental conditions in the current work can be compared with previous work, as shown in Table 3. In the current work a distinctly higher density difference, filling fraction, and angular velocity are used. The latter complicates the use of a single-sided drive that would enable the use of an open-ended tube and observation of cast growth during centrifugation. Submicron-sized particles were used only once before, namely by Sambuichi et al. (1991), who used a Hara Gairome Clay. In all studies, good agreement was obtained between experiment and simulation. It must be realized, however, that Sambuichi et al. (1987, 1991) used gravitational settling data to obtain an expression for the sedimentation coefficient s and did not base their model on Stokes' law.

Conclusion

In centrifugal casting distinct phases develop in time depending on the value of the filling fraction ζ. For a filling fraction ζ smaller than unity, these are a clear supernatant, a suspension phase, and the cast layer. For ζ equal to unity, a supernatant phase will not develop. Concentration gradients will not develop in any phase if diffusion can be neglected, which is the case in most practical situations.

Cast growth in centrifugal casting can be described satisfactorily from a condensed model combining *Kynch*-theory for the movement of the suspension–cast boundary with the appropriate expressions for the particle velocity and the equation of continuity for the suspension phase.

For unhindered settling, analytical solutions were found for all important process parameters. For hindered settling a straightforward numerical procedure proved useful. The agreement between the results from our condensed model and experiments in which submicron-sized particles were compacted into a cast proved satisfactory. Because particles were on the order of 10^6–10^9 (by volume) smaller than in the earlier experiments of Baron and Wajc (1979) and Schaflinger and Stibi (1987), this result is a useful extension of the validity of the current models and supports the important assumption that a hard-sphere approach can be used for particles of submicron size.

Table 3. Comparison of Measurement Conditions for Relative Density Difference ϵ [$\epsilon = (\rho_s - \rho_L)/\rho_L$], Initial Suspension Concentration ϕ_0, Particle Radius a_p, Angular Velocity ω, and Filling Fraction ζ*

Researchers	ϵ	ϕ_0	a_p (μm)	ω (rad/s)	ζ	Det. δ
Baron and Wajc (1979)	0.866	0.50	35	105	0.81	*p*
Schaflinger and Stibi (1987)	0.011–1.32	0.10	62–225	50–65	0.42–0.98	*p*
Sambuichi et al. (1987)	1.43–1.71	0.11–0.20	$\approx$ 2–10	162–324	0.37	*c*
Sambuichi et al. (1991)	0.133–1.71	0.09–0.30	0.2–4.2	84–231	0.37–0.53	*p*
Present work	2.97	0.20	0.2	344–612	1	*s*

*Cast thickness δ was either determined photographically during centrifugation (*p*), calculated from suspension concentration (*c*), or measured with a sliding gauge (*s*).

Acknowledgments

This work was supported financially by the Dutch Technology Foundation (NWO/STW). The authors thank Dr. M. H. G. Duits (Rheology Group, Faculty of Applied Physics, University of Twente) for help in measuring the liquid viscosity, and Dr. ir. B. C. Bonekamp (Netherlands Energy Research Foundation ECN) for useful discussions during preparation of the manuscript.

Literature Cited

Anestis, G., and W. Schneider, "Application of the Theory of Kinematic Waves to the Centrifugation of Suspensions," *Ing. Arch.*, **53**, 399 (1983).

Bachmann, P. K., P. Geittner, E. Krafczyk, H. Lydtin, and G. Romanowski, "Shape Forming of Synthetic Silica Tubes by Layerwise Centrifugal Deposition," *Amer. Ceram. Soc. Bull.*, **68**, 1826 (1989).

Baron, G., and S. Wajc, "Behinderte Sedimentation in Centrifugen," *Chem. Ing. Tech.*, **51**, 333 (1979).

Bowen, T. J., and A. J. Rowe, *An Introduction to Ultracentrifugation*, Wiley-Interscience, London (1970).

Concha, F., and E. R. Almendra, "Settling Velocities of Particulate Systems: 2. Settling Velocities of Suspensions of Spherical Particles," *Int. J. Miner. Proc.*, **6**, 31 (1979).

Fujita, H., *Mathematical Theory of Sedimentation Analysis*, Academic Press, New York (1962).

Fukui, Y., "Fundamental Investigation of Functionally Gradient Material Manufacturing System Using Centrifugal Force," *JSME Int. J. Ser. III*, **34**, 144 (1991).

Greenspan, H. P., "On the Centrifugal Separation of a Mixture," *J. Fluid Mech.*, **127**, 91 (1983).

Happel, J., and H. Brenner, *Low Reynolds Number Hydrodynamics*, Prentice Hall, Englewood Cliffs, NJ (1965).

Hong, C. W., "New Concept for Simulating Particle Packing in Colloidal Forming Processes," *J. Amer. Ceram. Soc.*, **80**, 2517 (1997).

Jones, F. R., "Centrifugal Casting," *Handbook of Polymer-Fibre Composites*, F. R. Jones, Ed., Polymer Science and Technology Series, Longman Scientific & Technical, New York, p. 144 (1994).

Kang, C. G., and P. K. Rohatgi, "Transient Thermal Analysis of Solidification in a Centrifugal Casting for Composite Materials Containing Particle Segregation," *Metall. Mater. Trans. B*, **27B**, 277 (1996).

Kynch, G. J., "A Theory of Sedimentation," *Trans. Faraday Soc.*, **48**, 166 (1952).

Lamm, O., "Die Differentialgleichung der Ultrazentrifugierung," *Arkiv. Mat., Astron., Fys.*, **21B**,1 (1929).

Lange, F. F., and K. T. Miller, "Pressure Filtration: Consolidation Kinetics and Mechanics," *Amer. Ceram. Soc. Bull.*, **66**, 1498 (1987).

Nijmeijer, A., C. Huiskes, N. G. M. Sibelt, H. Kruidhof, and H. Verweij, "The Preparation of Tubular Membrane Supports by Centrifugal Casting," *Amer. Ceram. Soc. Bull.*, **77**, 95 (1998).

Northcott, L., and V. Dickin, "The Influence of Centrifugal Casting (Horizontal Axis) upon the Structure and Properties of Metals," *J. Inst. Metals*, **70**, 301 (1944).

Perry, R. H., and D. W. Green, *Perry's Chemical Engineers' Handbook*, Int. Ed., McGraw-Hill, New York (1984).

Probstein, R. F., *Physicochemical Hydrodynamics, An Introduction*, Butterworths, Boston (1989).

Ring, T. A., *Fundamentals of Ceramic Powder Processing and Synthesis*, Academic Press, San Diego (1996).

Royer, A., "Horizontal Centrifugation: A Technique of Foundry Well Adapted to the Processing of High Reliability Pieces," *J. Mater. Shaping Tech.*, **5**, 197 (1988).

Russel, W. B., D. A. Saville, and W. R. Schowalter, *Colloidal Dispersions*, Cambridge Univ. Press, Cambridge (1989).

Sambuichi, M., H. Nakakura, K. Osasa, and F. M. Tiller, "Theory of Batchwise Centrifugal Filtration," *AIChE J.*, **33**, 109 (1987).

Sambuichi, M., H. Nakakura, and K. Osasa, "Zone Settling of Concentrated Slurries in a Centrifugal Field," *J. Chem. Eng. Jpn.*, **24**, 489 (1991).

Schachman, H. K., *Ultracentrifugaton in Biochemistry*, Academic Press, New York (1959).

Schaflinger, U., and H. Stibi, "On Centrifugal Separation of Suspensions in Cylindrical Vessels," *Acta Mech.*, **67**, 163 (1987).

Tiller, F. M., and N. B. Hsyung, "Unifying the Theory of Thickening, Filtration, and Centrifugation," *Water Sci. Technol.*, **28**, 1 (1993).

Ungarish, M., *Hydrodynamics of Suspensions: Fundamentals of Centrifugal and Gravity Separation*, Springer-Verlag, Berlin (1993).

Westerterp, K. R., W. P. M. van Swaaij, and A. A. C. M. Beenackers, *Chemical Reactor Design and Operation*, 2nd ed., Wiley, Chichester, U.K. (1987).

Appendix: Derivation of the Correction Factor for Hindered Settling

Concha and Almendra (1979) describe settling velocities of suspensions of spherical particles. From their expressions the correction factor for hindered settling is derived for $\{Re = 2\rho_L \upsilon a_p \eta^{-1}\} \to 0$. Here, particle velocity υ is based on Eq. 14 in the main text. The equations used by Concha and Almendra are indicated by square brackets in this Appendix. For batch settling, the settling velocity of solid particles υ_s is given as a function of the volumetric particle concentration ϕ and the relative particle-fluid velocity u (Eq. 34):

$$\upsilon_s = (1-\phi)u. \tag{A1}$$

Implementation of Eqs. 14, 15, and 32 into Eq. A1 results in

$$\upsilon_s = 10.26(1-\phi)\frac{\eta}{\rho_L}\frac{f_1}{a_p}\left(\left(1+0.0921\cdot 4\cdot\left(\frac{3}{2}\right)^{1/2} Re^{1/2} f_2\right)^{1/2} - 1\right)^2. \tag{A2}$$

Here we have replaced the acceleration due to gravity g by the acceleration in a centrifugal field $\omega^2 r$. From the data of Table 1 with $r = r_0$, a value of $Re = 1\cdot 10^{-5}$ follows, and thus the transformation $\{x \to 0\} \to \{(1+x)^{1/2} \to (1+1/2\,x)\}$ can be made with an error of 0.03% in υ_s, after which Eq. 2 simplifies to

$$\upsilon_s = 10.26(0.0921)^2 \frac{8}{3}(1-\phi)a_p^2 f_1 f_2^2 \omega^2 r \Delta\rho\eta^{-1}. \tag{A3}$$

Parameters f_1 and f_2 are given by Eqs. 39, 40:

$$f_1 = \frac{(1-\phi)^2(1+0.75\phi^{1/3})}{(1-\phi+1.2\phi^{2/3})^{3/2}(1-1.45\phi)^{1.83}}$$

$$f_2 = \frac{(1-\phi+1.2\phi^{2/3})^{3/4}(1-1.45\phi)^{1.83}}{(1-\phi)(1+0.75\phi^{1/3})}. \tag{A4}$$

The correction factor $h(\phi)$ equals the ratio of υ_s (Eq. A3) over υ (Eq. 14). After implementation of Eq. A4 into Eq. A3 and allowing for an error of 4%, $h(\phi)$ can be calculated to be

$$h(\phi) = \frac{(1-\phi)(1-1.45\phi)^{1.83}}{(1+0.75\phi^{1/3})}. \tag{A5}$$

Manuscript received Jan. 13, 1998, and revision received Apr. 13, 1998.